

# Boundary Layer Slip Flow and Heat Transfer over an Exponential Shrinking Sheet

RAJESH SHARMA

Department of Mathematics, National Institute of Technology Hamirpur,  
Hamirpur, Himachal Pradesh, INDIA, 177005  
raj.juit@gmail.com

*Abstract:* - The boundary layer slip flow with heat transfer over a permeable exponential shrinking sheet with mass flux at the boundary is studied. Using similarity transformation in exponential form, similarity equations are obtained which are then solved numerically by finite difference method using MATLAB solver bvp4c. The numerical results show that dual solutions exist beyond a certain value of mass suction and the range of mass suction parameter for which the solution exists expands with the velocity slip parameter. A stability analysis has been conducted to show that first solution branch is stable while the second is always unstable.

*Key-Words:* -Heat transfer, dual solutions, slip flow, shrinking sheet, stability analysis

## 1 Introduction

The phenomena over stretching sheet have a wide range of applications in aerospace, production of polymers, metal casting. Metal or more commonly an alloy, is heated till the molten state is achieved and then it is transferred into a die. A state of liquid contraction is achieved when a melting issue from a die comes out so it drops its heat and contracts on cooling. The desired product is obtained by stretching the hot metal issue from the die. The atoms of the metal lose energy on further cooling and loss of latent heat of fusion and closely bound together in a regular structure. The nature of the final product depends on the process of stretching and the rate of heat transfer at the surface.

The study of boundary layer flow due to a stretching sheet is initiated by Crane [1]. He obtained an analytical solution by assuming the linear velocity variation. Many researchers e.g. Gupta and Gupta [2], Grubka and Bobba [3], Vajravelu [4], Ali and Mehmood [5], Ishak et al. [6], Kazem et al. [7], Sharma [8], Sharma et al. [9] extended the work of Crane [1] under different physical situations by including the effect of heat transfer analysis. Vajravelu [4] examined the case in which the wall is being stretched with a variable velocity and the free-stream velocity is constant. Sharma [8] investigated the unsteady flow with heat transfer past a stretching surface embedded in a porous medium with viscous

dissipation and heat source effect using element free Galerkin method. Sharma et al. [9] studied the nanofluid flow driven by a stretching sheet including the effect of partial slip condition on the boundary.

Wang [10] was the first to investigate but gave only a little information about the flow past an unsteady shrinking sheet film. Later, shrinking sheet problem was investigated by Miklavcic and Wang [11], they established the existence and uniqueness criteria for similarity solutions of this problem if to restrain vorticity, sufficient suction on the surface is applied. Further, this problem was investigated by Fang and Zhang [12], Cortell [13], Merkin and Kumaran [14], Sharma et al. [15] and many others. Sharma et al. [16] have investigated the stagnation point flow of a micropolar fluid over a stretching/shrinking sheet with second-order velocity slip. Recently, Fauzi et al. [17] have studied the flow and heat transfer over a stretching and shrinking sheet with slip and convective boundary condition.

In most of the circumstances, fluid normally sticks to the boundary and no-slip condition is consistent with the flow problem. Many fluids with particulates, such as emulsions, suspensions, foams, polymer solution etc., with slip between the fluid and the surface [18]. In this article, we have investigated the boundary layer flow and heat transfer problem over an exponentially shrinking sheet with thermal slip effects as proposed by Beavers and Joseph

[19]. Analytical solution is hard to find out because of nonlinearity of the mathematical model. Therefore, in this study, numerical simulation has been performed using MATLAB boundary value problem (BVP) solver bvp45.

## 2 Problem formulation

Alaminar boundary layer flow of a viscous and incompressible fluid over a permeable exponentially shrinking sheet coinciding with the plane  $y=0$  is considered. Flow is constrained in the region  $y \geq 0$  as shown in Fig. 1. Wall shrinks by keeping the origin fixed on applying two equal and opposite force along sheet towards origin. Further, let the mass flux velocity is  $V_w(x)$  with  $V_w(x) > 0$  for injection or withdrawal of the fluid and  $V_w(x) < 0$  for suction.

Under these assumptions the governing equations of the flow in dimensions are as follows:

$$\frac{\partial u}{\partial x} + \frac{\partial v}{\partial y} = 0 \tag{1}$$

$$u \frac{\partial u}{\partial x} + v \frac{\partial u}{\partial y} = \nu \frac{\partial^2 u}{\partial y^2} \tag{2}$$

$$u \frac{\partial T}{\partial x} + v \frac{\partial T}{\partial y} = \alpha \frac{\partial^2 T}{\partial y^2} \tag{3}$$

where  $u$  and  $v$  are the velocity components in the  $x$  and  $y$  directions,  $T$  is the fluid temperature,  $\alpha$  is the thermal diffusivity,  $\nu$  is the kinematic viscosity. The corresponding boundary conditions are:

$$v = V_w(x), \quad u = U + Nv \frac{\partial u}{\partial y}, \quad T = T_w + D \frac{\partial T}{\partial y} \quad \text{at } y = 0 \tag{4}$$

$$u \rightarrow 0, \quad T \rightarrow T_\infty \quad \text{as } y \rightarrow \infty$$

Where  $V_w(x) = V_0 \exp(x/2L_1)$  mass flux velocity,  $U = -U_0 \exp(x/L_1)$  is the shrinking velocity,  $T_w = T_0 \exp(x/2L_1)$  is the variable temperature at the sheet. Here  $L_1, U_0, T_0$  and  $V_0$  are the length, velocity, temperature and mass flux velocity respectively with  $V_0 < 0$  for suction and  $V_0 > 0$  for injection. More, we assume that  $N = N_1 \exp(-x/2L_1)$  and  $D = D_1 \exp(-x/2L_1)$  are the slip velocity factor and the thermal slip factor respectively which varies with  $x$ , where  $N_1$  and  $D_1$  are the initial values of

velocity and thermal slip factor respectively [20].  $N = D = 0$  is the no slip case.

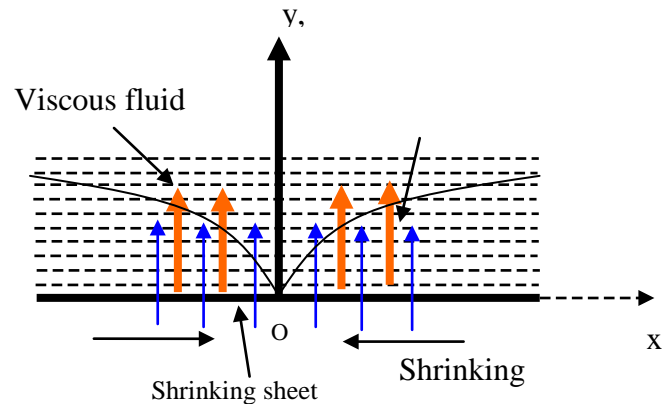


Fig. 1: Physical Model and Coordinate System

Now we introduce the following similarity variables (see Mukhopadhyay and Gorla [21]),

$$\eta = y \sqrt{\frac{U_0}{2\nu L_1}} \exp(x/2L_1), \quad u = U_0 \exp(x/L_1) f'(\eta),$$

$$v = -\sqrt{\frac{\nu U_0}{2L_1}} \exp(x/2L_1) [f(\eta) + \eta f'(\eta)] \tag{5}$$

$$T = T_0 \exp(x/2L_1) \theta(\eta)$$

where prime denotes differentiation with respect to  $\eta$ . Substituting (5) into Eqs. (2) and (3), we obtain the following ordinary differential equations

$$f''' + ff'' - 2f'^2 = 0 \tag{6}$$

$$\frac{1}{Pr} f'' + (f\theta' - f'\theta) = 0 \tag{7}$$

with boundary conditions

$$f(0) = s, \quad f'(0) = -1 + \lambda f''(0), \quad \theta(0) = 1 + \delta \theta'(0)$$

$$f'(\eta) \rightarrow 0, \quad \theta(\eta) \rightarrow 0 \quad \text{as } \eta \rightarrow \infty \tag{8}$$

Here  $\lambda = N_1 \sqrt{U_0 \nu / 2L_1} (> 0)$  is the velocity slip parameter,  $\delta = D_1 \sqrt{U_0 / 2\nu L_1} (> 0)$  is the thermal slip parameter,  $s = -V_0 \sqrt{U_0 / 2\nu L_1}$  is the suction ( $s > 0$ ) or blowing ( $s < 0$ ) parameter and  $Pr = \nu / \alpha$  is the Prandtl number.

Skin friction coefficient  $C_f$  and the local Nusselt number  $Nu$  are defined as

$$C_f = \frac{\mu}{\rho [U_0 \exp(x/L_1)]^2} \left( \frac{\partial u}{\partial y} \right)_{y=0}, \tag{9}$$

$$Nu = \frac{L_1}{T_0 \exp(x/2L_1)} \left( -\frac{\partial T}{\partial y} \right)_{y=0}$$

Using (5) into (12), we get

$$f''(0) = (2Re)^{1/2} C_f, \quad \theta'(0) = -(2/Re)^{1/2} Nu \tag{10}$$

Where  $Re = (U_0 L_1 / \nu) \exp(x/L_1)$  is the Reynolds Number.

### 3 Method of Solution

A boundary value problem is obtained using a nonlinear set of differential Eqs. (6) and (7), along with the boundary conditions (8) and is solved numerically by finite difference method with fourth order accuracy using MATLAB solver bvp45. In this approach, problem is converted into an initial value problem (IVP) by introducing new variables. In this method, a suitable finite value of  $\eta_\infty$  (where  $\eta_\infty$  correspond to  $\eta \rightarrow \infty$ ) is chosen to obtain asymptotically converged solution with the maximum residuals less than  $10^{-10}$  for a given set of parameters. For computational purposes,  $\eta_\infty$  has been fixed as 4. It is sufficient to achieve asymptotically the free stream boundary conditions for all values of the considered parameters.

First order differential equations are obtained as

$$f' = y_1, y_1' = y_2, y_2' = 2y_1^2 - f y_2 \tag{11}$$

$$\theta' = y_3, y_3' = -Pr(f y_3 - y_1 \theta) \tag{12}$$

with the boundary conditions

$$f(0) = s, y_1(0) = -1 + \lambda y_2(0), \theta(0) = 1 + \delta y_3(0) \tag{13}$$

Eqs. (11) and (12) with Eq. (13) forms an IVP and we need the values of  $y_2(0)$  and  $y_3(0)$ . The initial guess values for  $y_2(0)$  and  $y_3(0)$  are choose in such a way that the solution must satisfy the conditions (8). It is found that within a certain range of S dual solutions are obtained with different initial guess values.

However, in order to validate the present method of solution, we compare the present results with ones from the open literature, we consider the boundary layer problem of a viscous (regular) and incompressible fluid flow with heat transfer near the stagnation-point of an impermeable shrinking sheet,

which are given by the following equations (see Wang [22])

$$f''' + f f'' - f'^2 + 1 = 0 \tag{14}$$

$$\theta'' + (f \theta' - \theta f') = 0 \tag{15}$$

subject to the boundary conditions

$$f(0) = 0, f'(0) = \varepsilon, \theta(0) = 1 \tag{16}$$

$$f'(\eta) \rightarrow 1, \theta(\eta) \rightarrow 0 \text{ as } \eta \rightarrow \infty$$

Table 1 shows the comparison of the present numerical results with those of Wang [22] for the problem defined in Eqs. (14) to (16), which shows a quite good agreement. Therefore, we believe that the present results are correct.

**Table 1.** Comparison of present results with those of Wang [22]

$\varepsilon$	Wang [22]		Present results	
	Upper Branch	Lower Branch	Upper Branch	Lower Branch
2.0	-1.88731		-1.887306	
1.0	0		0	
0.5	0.71330		0.713295	
0.0	1.232588		1.232588	
-0.25	1.40224		1.495670	
-0.5	1.49567		1.495670	
-1.0	1.32882	0	1.328817	0
-1.15	1.08223	0.116702	1.082232	0.1167022
-1.2			0.932473	0.233650
-1.2465	0.55430		0.554297	0.584281
-1.24657			0.564015	

### 4 Flow Stability

As Merkin [23] and Weidman et al. [24] suggested, the stability of flow can be checked by considering the unsteady model of examined problem as follows:

$$\frac{\partial u}{\partial x} + \frac{\partial v}{\partial y} = 0 \tag{17}$$

$$\frac{\partial u}{\partial t} + u \frac{\partial u}{\partial x} + v \frac{\partial u}{\partial y} = \nu \frac{\partial^2 u}{\partial y^2} \tag{18}$$

$$\frac{\partial T}{\partial t} + u \frac{\partial T}{\partial x} + v \frac{\partial T}{\partial y} = \alpha \frac{\partial^2 T}{\partial y^2} \tag{19}$$

where t is the time.

We assume that the initial & boundary conditions are given by

$$\begin{aligned}
 t < 0: v = 0, u = 0, T = 0 \text{ for any } x, y \\
 t \geq 0: v = V_w(x), u = U + Nv \frac{\partial u}{\partial y}, T = T_w + D \frac{\partial T}{\partial y} \text{ at } y = 0 \\
 u \rightarrow 0, T \rightarrow T_\infty \text{ as } y \rightarrow \infty
 \end{aligned}
 \tag{20}$$

Using the following similarity variables,

$$\begin{aligned}
 \eta = y \sqrt{\frac{U_0}{2\nu L_1}} \exp(x/2L_1), u = U_0 \exp(x/L_1) f'(\eta, \tau), \\
 v = -\sqrt{\frac{\nu U_0}{2L_1}} \exp(x/2L_1) [f(\eta, \tau) + \eta f'(\eta, \tau)] \\
 T = T_0 \exp(x/2L_1) \theta(\eta, \tau), \tau = \frac{U_0}{2L_1} \exp(x/L_1) t
 \end{aligned}
 \tag{21}$$

Substituting (21) into Eqs. (18) and (19), we obtain the following differential equations

$$f''' + f f'' - 2f'^2 - \frac{\partial f'}{\partial \tau} (1 + 2\tau f') = 0 \tag{22}$$

$$\frac{1}{Pr} \theta'' + (f \theta' - f' \theta) - \frac{\partial \theta}{\partial \tau} (1 + 2\tau f') = 0 \tag{23}$$

and the corresponding boundary conditions (20) become

$$\begin{aligned}
 \tau < 0: f = 0, f' = 0, \theta = 0 \text{ for any } \eta \\
 \tau \geq 0: f(0) = s, f'(0) = -1 + \lambda f''(0), \theta(0) = 1 + \delta \theta'(0) \\
 f'(\eta) \rightarrow 0, \theta(\eta) \rightarrow 0 \text{ as } \eta \rightarrow \infty
 \end{aligned}
 \tag{24}$$

To test stability of the steady flow solution,  $f(\eta, 0) = f_0(\eta)$  and  $\theta(\eta, 0) = \theta_0(\eta)$  satisfying the boundary-value problem (6)-(8), we write (see Weidman *et al.* [24]),

$$\begin{aligned}
 f(\eta, \tau) = f_0(\eta) + e^{-\gamma \tau} F(\eta, \tau) \\
 \theta(\eta, \tau) = \theta_0(\eta) + e^{-\gamma \tau} G(\eta, \tau)
 \end{aligned}
 \tag{25}$$

where  $F(\eta, \tau)$  and  $G(\eta, \tau)$  are small relative to  $f_0(\eta)$  and  $\theta_0(\eta)$  respectively, and  $\gamma$  is the eigenvalue. Substituting the expression (25) into Eqs. (22) and (23), we obtained the following equations

$$\begin{aligned}
 \frac{\partial^3 F}{\partial \eta^3} + f_0 \frac{\partial^2 F}{\partial \eta^2} + F \frac{\partial^2 f_0}{\partial \eta^2} - 4 \frac{\partial f_0}{\partial \eta} \frac{\partial F}{\partial \eta} + \\
 \gamma \left( 1 + 2\tau \frac{\partial f_0}{\partial \eta} \right) \frac{\partial F}{\partial \eta} - \left( 1 + 2\tau \frac{\partial f_0}{\partial \eta} \right) \frac{\partial^2 F}{\partial \eta \partial \tau} = 0
 \end{aligned}
 \tag{26}$$

$$\begin{aligned}
 \frac{\partial^2 G}{\partial \eta^2} + f_0 \frac{\partial G}{\partial \eta} + F \frac{\partial \theta_0}{\partial \eta} - \frac{\partial f_0}{\partial \eta} \frac{\partial G}{\partial \eta} - \theta_0 \frac{\partial F}{\partial \eta} \\
 + \gamma G \left( 1 + 2\tau \frac{\partial f_0}{\partial \eta} \right) - \left( 1 + 2\tau \frac{\partial f_0}{\partial \eta} \right) \frac{\partial G}{\partial \tau} = 0
 \end{aligned}
 \tag{27}$$

subject to the following boundary conditions

$$\begin{aligned}
 F(0, \tau) = 0, \frac{\partial F}{\partial \eta}(0, \tau) = \lambda \frac{\partial^2 F}{\partial \eta^2}(0, \tau), \\
 G(0, \tau) = \delta \frac{\partial G}{\partial \eta}(0, \tau) \\
 \frac{\partial F}{\partial \eta}(\eta, \tau) \rightarrow 0, G(\eta, \tau) \rightarrow 0 \text{ as } \eta \rightarrow \infty
 \end{aligned}
 \tag{28}$$

We investigate the stability of the steady flow solution  $f_0(\eta)$  and  $\theta_0(\eta)$  by solving the corresponding steady linear eigenvalue problem

$$\frac{\partial^3 F}{\partial \eta^3} + f_0 \frac{\partial^2 F}{\partial \eta^2} + F \frac{\partial^2 f_0}{\partial \eta^2} - 4 \frac{\partial f_0}{\partial \eta} \frac{\partial F}{\partial \eta} + \gamma \frac{\partial F}{\partial \eta} = 0 \tag{29}$$

$$\frac{\partial^2 G}{\partial \eta^2} + f_0 \frac{\partial G}{\partial \eta} + F \frac{\partial \theta_0}{\partial \eta} - \frac{\partial f_0}{\partial \eta} \frac{\partial G}{\partial \eta} - \theta_0 \frac{\partial F}{\partial \eta} + \gamma G = 0 \tag{30}$$

With the boundary conditions

$$\begin{aligned}
 F(0) = 0, F'(0) = \lambda F''(0), G(0) = \delta G'(0) \\
 F'(\eta) \rightarrow 0, G(\eta) \rightarrow 0 \text{ as } \eta \rightarrow \infty
 \end{aligned}
 \tag{31}$$

Numerical values of  $f_0(\eta)$  and  $\theta_0(\eta)$  obtained from the solution of (6) and (7), for particular value of  $\lambda$  and  $\delta$ , an infinite set of eigenvalues are obtained from the solution of (29) and (30). The stable flow is determined by positive minimum eigenvalue. The sign of smallest eigenvalue  $\gamma$  determines the stability of steady flow solution  $f_0(\eta)$  and  $\theta_0(\eta)$ . Harris *et al.* [25] explained that if boundary condition on  $F(\eta)$  or  $G(\eta)$  is relaxed and value of  $\gamma$  is fixed, the range of possible eigenvalues can be determined.

## 5 Results and discussion

The governing boundary value problem defined by ordinary differential equations (6) and (7), along with the boundary conditions (8) are solved numerically using MATLAB routine BVP solver `bvp4c` for various set of values of the physical parameters. To solve this BVP with MATLAB routine BVP solver, we need the initial guess values of  $f''(0)$  and  $\theta'(0)$ . It is found that with different initial guess will result in two different solutions. With the earlier analysis for the shrinking sheet case (Miklavcic and Wang [11]; Sharma *et al.* [15]; Sharma *et al.* [16]) duality nature of the solution is consistent.

The effect of velocity slip parameter  $\lambda$  and thermal slip parameter  $\delta$  with different values of Variation of  $S$  on the reduced skin friction coefficient  $f''(0)$  and

the reduced local Nusselt number  $-\theta'(0)$  are presented in Figs. 2-3 and Fig. 4. It is observed that when  $s$  is smaller than the critical value  $s_c (> 0)$ , there is no solution and when  $s > s_c$ , there are two solutions. Based on our computations, the critical value of  $s$  decreases as  $\lambda$  increases and is independent of the values of  $\delta$ . Hence, velocity slip parameters widen the range of  $s$  for which the solution exists.

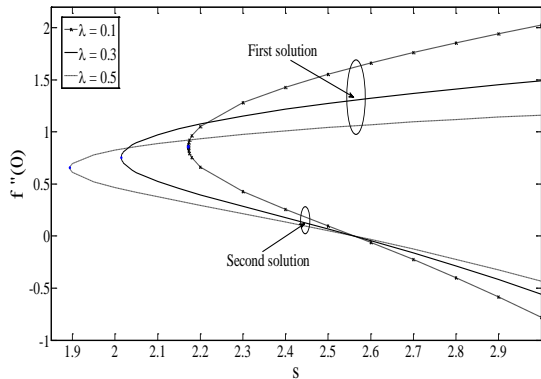


Fig. 2: Graph of  $f''(0)$  with  $s$  for various values of  $\lambda$

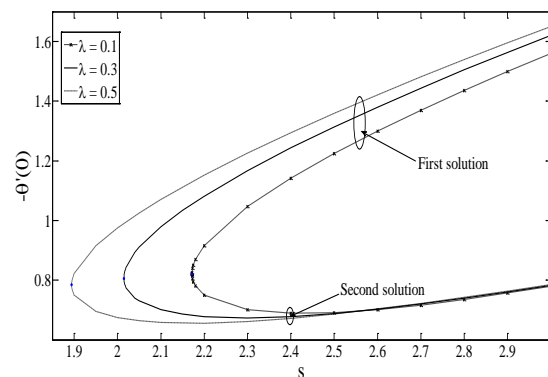


Fig. 3: Graph of  $-\theta'(0)$  with  $s$  for various values of  $\lambda$

In Figs. 2-3,  $f''(0)$  decreases but  $-\theta'(0)$  increases with increasing  $\lambda$ , for the first solution. Thus, the surface shear stress decreases but the heat transfer at the surface increases with  $\lambda$ . The second solution shows quite different and complicated behaviors compared with the first solution. For the second solution, with the increase in  $\lambda$ , both  $f''(0)$  and  $-\theta'(0)$  decrease, while for  $s > 2.54$  the pattern is opposite. In Figs. 4, it is seen that for both solution branches i.e. first & second solution, with lower values of  $\delta$ , the value of  $-\theta'(0)$  is consistently

higher.

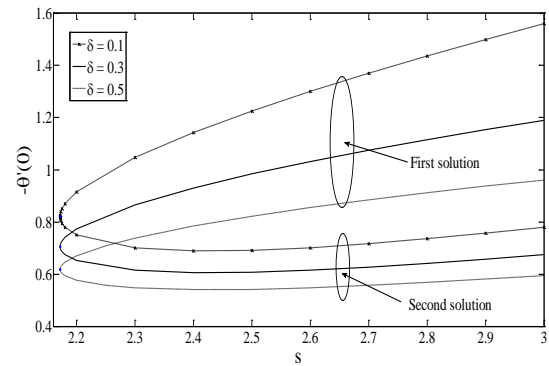


Fig. 4: Graph of  $-\theta'(0)$  with  $s$  for various values of  $\delta$

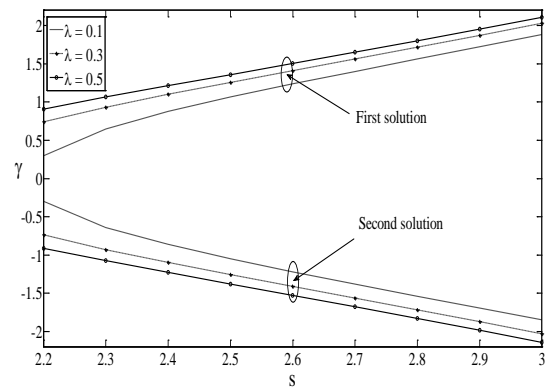


Fig. 5: Graph of  $\gamma$  with  $s$  for various values of  $\lambda$

Linear stability of the steady flow solution has been examined according to Merkin [23] and Weidman et al. [24]. According to Merkin [23] and Weidman et al. [24], the sign of the smallest eigenvalue determines the stability of the obtained solution. The positive minimum eigenvalue determines the stable flow. Based on this approach, we have converted the problem to eigenvalue problem and find out the minimum eigenvalue for both the solution shown in figure 5 & 6. For first solutions, the eigenvalues are always positive, while negative for second solutions. Thus, we conclude that the second solutions are linearly unstable, while first solutions are linearly stable for these particular parameter values. It is also observed from Figs. 5 & 6 that stability of first solution branch increases with the increase of  $\lambda$  and  $s$ , while  $\delta$  has no effect on flow stability.

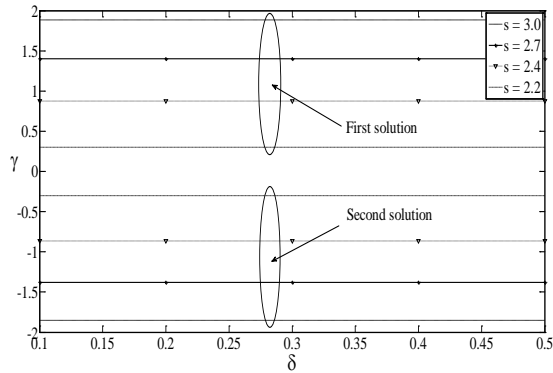


Fig. 6: Graph of  $\gamma$  with  $s$  for various values of  $\delta$

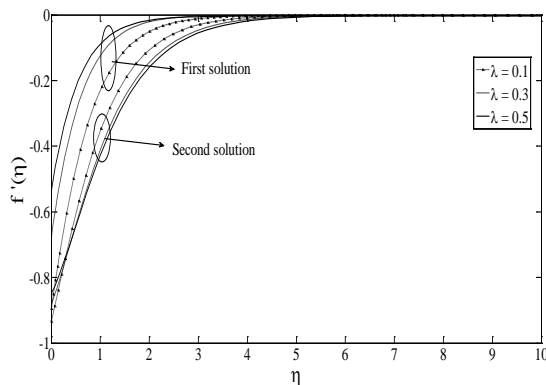


Fig. 7:  $f'(\eta)$  for various values of  $\lambda$

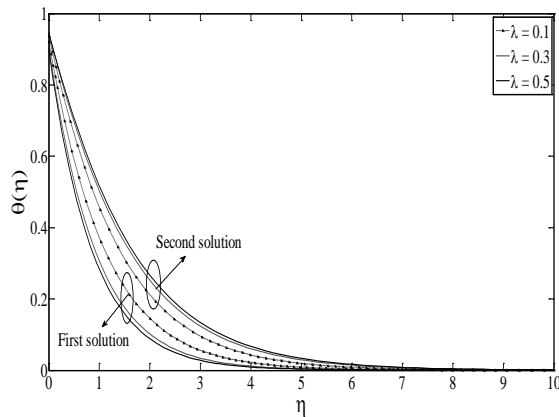


Fig. 8:  $\theta(\eta)$  for various values of  $\lambda$

Figure 7-8 exhibit the velocity and temperature profiles respectively for the velocity slip parameter  $\lambda$ . The free stream boundary conditions (8) are satisfied asymptotically in these figures, which validates the obtained numerical results. It is also noticed that thermal as well as momentum boundary layer thickness for the first solution is lower than that of the second solution. Figure 7 shows for the 1<sup>st</sup> solution, an increase in the velocity of the fluid throughout the boundary layer region is observed,

with an increase in the velocity slip parameter  $\lambda$ , while for the 2<sup>nd</sup> solution, near the wall, the velocity increases with  $\lambda$  and away from the wall, reverse pattern is observed. We also observed that, due to increasing value of  $\lambda$  the momentum boundary layer become thinner for the first solution and opposite nature is observed for the 2<sup>nd</sup> solution. The temperature at a point near the wall decreases for an increase in  $\lambda$  for the 1<sup>st</sup> solution and for the 2<sup>nd</sup> solution, the nature is reversed which is shown in Fig.8.

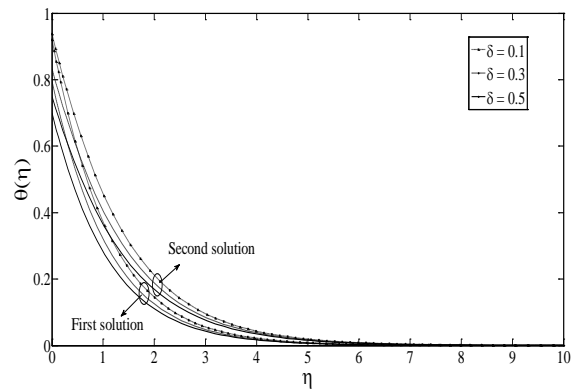


Fig. 9:  $\theta(\eta)$  for various values of  $\delta$

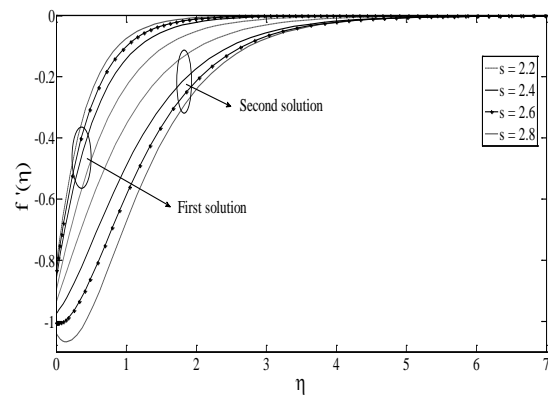


Fig. 10:  $f'(\eta)$  for various values of  $s$

Figure 9 gives the variation of temperature profile within the boundary layer with thermal slip parameter. For both first and second solutions the temperature profile shows a smoothly decreasing pattern with  $\eta$ . It is also observed that for both the solutions, the temperature distribution decreases with the increase in thermal slip parameter. Further, it is noted that the change in temperature is higher near the sheet with thermal slip parameter, but very less away from the sheet. As seen in Fig. 4, temperature is found to decrease because thermal slip parameter reduces the rate of heat transfer. Figure 10 depict the variation in velocity with mass suction. It is noted

that mass suction parameter increases the velocity for first solution branch, while reverse pattern is seen for the second solution.

## 6 Conclusions

In summary, the mathematical model of viscous flow and heat transfer past a permeable exponentially shrinking sheet with mass flux at the wall and slip effect has been solved numerically using MATLAB BVP solver bvp4c to show the influence of velocity slip parameter  $\lambda$ , thermal slip parameter  $\delta$  and mass suction parameter  $s$ . It is found that dual solutions exist beyond a certain range of mass suction parameter and the range of mass suction parameter for which the solution exists expands with the velocity slip parameter. Linear stability of first solution is noted while second solution seems to be unstable. The stability of flow increases with increasing mass suction parameter  $s$  and velocity slip parameter  $\lambda$ .

## Acknowledgements

The work was supported by Research Grants received from the SERB, DST, Govt. of India (Project Code: ECR/2016/000368).

## References:

1. L. J. Crane, Flow past a stretching plate, *J. Appl. Math. Phys. (ZAMP)*, Vol. 21, 1970, pp. 645-647.
2. P. S. Gupta and A. S. Gupta, Heat and mass transfer on a stretching sheet with suction or blowing, *Can. J. Chem. Eng.*, Vol. 55, 1977, pp. 744-746.
3. L. J. Grubka and K. M. Bobba, Heat transfer characteristics of a continuous, stretching surface with variable temperature, *Trans. ASME J. Heat Transfer*, Vol. 107, 1985, pp. 248-250.
4. K. Vajravelu, Viscous fluid over a non-linearly stretching sheet, *Appl. Math. Comput.*, Vol. 124, 2001, pp. 281-288.
5. A. Ali and A. Mehmood, Homotopy analysis of unsteady boundary layer flow adjacent to permeable stretching surface in a porous medium, *Commun. Nonlinear Sci. Numer. Simulat.*, Vol. 13, 2008, pp. 340-349.
6. A. Ishak, R. Nazar and I. Pop, "Heat transfer over an unsteady stretching permeable surface with

prescribed wall temperature," *Nonlinear Anal. Real World Appl.*, Vol. 10, 2009, pp. 2909-2913.

7. S. Kazem, M. Shaban and S. Abbasbandy, Improved analytical solutions to a stagnation-point flow past a porous stretching sheet with heat generation, *J. Franklin Inst.*, Vol. 348, 2011, pp. 2044-2058.
8. R. Sharma, Effect of viscous dissipation and heat source on unsteady boundary layer flow and heat transfer past a stretching surface embedded in a porous medium using element free Galerkin method, *Appl. Math. Comput.*, Vol. 219, 2012, pp. 976-987.
9. R. Sharma, A. Ishak and I. Pop, Partial slip flow and heat transfer over a stretching sheet in a nanofluid, *Mathematical Problem in Engineering*, Vol. 2013, 2013, Article ID 724547, 7 pages.
10. Y. Wang, Liquid film on an unsteady stretching sheet, *Quart. Appl. Math.*, Vol. 48, 1990, pp. 601-610.
11. M. Miklavcic and C. Y. Wang, Viscous flow due to a shrinking sheet, *Quart. Appl. Math.*, Vol. 64, 2006, pp. 283-290.
12. T. Fang and J. Zhang, "Closed-form exact solutions of MHD viscous flow over a shrinking sheet, *Commun. Nonlinear Sci. Numer. Simulat.*, Vol. 14, 2009, pp. 2853-2857.
13. R. Cortell, On a certain boundary value problem arising in shrinking sheet flows, *Appl. Math. Comput.*, Vol. 217, 2010, pp. 4086-4093.
14. J. H. Merkin and V. Kumaran, The unsteady MHD boundary-layer flow on a shrinking sheet, *Eur. J. Mech. B Fluids*, Vol. 29, 2010, pp. 357-363.
15. R. Sharma, A. Ishak, I. Pop, Stability analysis of magnetohydrodynamics stagnation-point flow towards a stretching/shrinking sheet, *Comp. Fluids*, Vol. 102, 2014, pp. 94-98.
16. R. Sharma, A. Ishak, I. Pop, Stagnation point flow of a micropolar fluid over a stretching/shrinking sheet with second-order velocity slip, *J. Aerospace Eng.*, Vol. 29, No. 5, 2016, 04016025.
17. E. L. A. Fauzi, S. Ahmad, I. Pop, Flow and heat transfer over a stretching and shrinking sheet with slip and convective boundary condition, *AIP Conf. Proc.*, Vol. 1830, 2017, 020019.
18. V. P. Shidlovskiy, *Introduction to the Dynamics of Rarefied Gases*. American Elsevier Publishing Company Inc, New York, 1967.
19. G. S. Beavers and D. D. Joseph, Boundary condition at a naturally permeable wall, *J. Fluid Mech.*, Vol. 30, 1967, pp. 197-207.

- 20.S. Mukhopadhyay and H. I. Andersson, Effects of slip and heat transfer analysis of flow over an unsteady stretching surface, *Heat Mass Transfer*, Vol. 45, 2009, pp. 1447–1452.
- 21.S. Mukhopadhyay and R. S. R. Gorla, Effects of partial slip on boundary layer flow past a permeable exponential stretching sheet in presence of thermal radiation, *Heat Mass Transfer*, Vol. 48, 2012, pp. 1773-1781.
- 22.C. Y. Wang, Stagnation flow towards a shrinking sheet, *Int. J. Non-Linear Mech.*, Vol. 43, 2008, pp. 377-382.
23. J. H. Merkin, On dual solutions occurring in mixed convection in a porous medium, *J. Eng. Math.*, Vol. 20, 1985, pp. 171-179.
- 24.P. D. Weidman, D. G. Kubitschek, A. M. J. Davis, The effect of transpiration on self-similar boundary layer flow over moving surface, *Int. J. Eng. Sci.*, Vol. 44, 2006, pp.730-737.
25. S. D. Harris, D. B. Ingham, I. Pop, Mixed convection boundary-layer flow near the stagnation point on a vertical surface in a porous medium: Brinkman model with slip, *Transp. Porous Med.*, Vol. 77, 2009, pp. 267–285.